Article

Complexity Study in Different States of Consciousness Using Brain Waves

Medha Basu* & Dipak Ghosh

Dept. of Physics, Sir C.V. Raman Centre for Physics and Music, Jadavpur Univ., India

Abstract

Human brain is the prime hub for carrying out all body and mind activities, by relaying information in form of electric waves across millions of neurosynaptic junctions. These electric waves represent the neural signals, which can be broadly classified into different frequency ranges, showing varied levels of dominance for different states of consciousness. In this study, during resting state of 7 voluntary participants, we have extracted and studied the complexity of three neural waves, delta (1 – 4 Hz), theta (4 – 8 Hz) and alpha (8 – 12 Hz) waves, which represent different states of consciousness. Linear techniques were first applied to study parameters like 'Spectral Power' and 'Hemispherical Power Asymmetry' in all three waves. Keeping in mind the non-linear nature of the extracted neural signals, it seemed more appropriate to use non-linear techniques of analysis, to efficiently capture the intrinsic fluctuation details of the time series. Multifractality and complexity of the different waves were computed and compared by the process of 'Multifractal Detrended Fluctuation Analysis' (MFDFA) for resting state. Approximate Entropy (ApEn) was computed to understand the predictability of the fluctuations in the neural waves. Statistical tools like One-way ANOVA, and Mahalanobis Distance were also computed to study the nature of significant difference between the three waves, in terms of each of these above-mentioned properties. All parameters were calculated for both left and right hemispherical sections of frontal, temporal, occipital and parietal lobes. Spectral power in all lobes showed prominently high values for delta waves, and overlapping lower values for theta and alpha waves. Complexity values showed a particular trend in most of the cases, showing highest value in delta, followed by alpha and theta. ApEn in all lobes showed highest values for alpha waves, followed by theta and delta. Power asymmetry and MW asymmetry parameters showed distinctly different behaviour for delta, theta, and alpha waves for most of the lobes. Statistical calculations on the computed parameters revealed different degrees of correlation for delta-theta, alpha-theta, and delta-alpha wave pairs. ANOVA revealed valid significant difference between delta-theta and alpha-theta waves in case of Spectral Power values, and between all three waves in case of ApEn values. Mahalanobis Distance between the three waves showed different trends of values for each of the above-mentioned properties. Results showed, parameters computed by linear methods (Spectral Power, and Power-Asymmetry) failed to reveal prominent distinction between all of the three waves, and certain

*Correspondence: Medha Basu, Senior Research Scholar, Dept. of Physics, Sir C.V. Raman Centre for Physics and Music, Jadavpur Univ., India. Email: medhabasu1996@gmail.com

amount of overlap was observed between computed values of alpha and theta waves in some lobes. Non-linear methods of analysis on the other hand, showed prominent trends of distinction between all three neural waves in all lobes, highlighting better efficiency of non-linear techniques to differentiate neural waves during resting state. The paper presents several new information and interesting points of distinction between delta, theta, alpha waves as revealed from non-linear studies, during resting state of the participants, which are manifestations of different states of consciousness.

Keywords: Brain wave, consciousness, complexity, delta wave, theta wave, alpha wave, resting state, distinction, asymmetry.

I. INTRODUCTION

Brain lobes and neural waves

Human neurocognition is one of the most complicated and difficult domains of study and research. Brain, cognition, and consciousness are intertwined areas which require detailed stringent analysis for proper understanding. After modifications through centuries, human brain has reached the state of maximum efficiency and development amongst all other species, with the highest capability of different aspects like decision making, creativity, memory, computation etc. Human brain can be broadly divided into four primary lobes, frontal [1] [2] [3], temporal [4] [5] [6], parietal [7] [8] [9] and occipital [10] [11], each with certain assigned functions to perform. Frontal lobe is primarily known for reasoning, analysis, computation, logic, decision-making etc. Temporal lobe is mostly associated with hearing, occipital lobe with vision and parietal lobe with sensation like touch, pain, temperature etc. It should be kept in mind here that these lobes are all interconnected with an intricate network of neurons, which are the unit cells of brain, forming the constructive and functional building blocks. Neurons are interconnected with synaptic junctions, which relay information from different parts of brain in form of electric signal potentials, bringing out a deep connectivity and synchronization within the entire brain, and connecting all lobes with one another.

Brain, one of the most complex systems of nature performs multiple functions incessantly throughout the day, even when the person is under a state of relaxation. Neural signals [12] have several frequency components, which show different levels of prominence for different activities. During deep sleep and drowsy state, delta wave (1 - 4Hz) [13] shows maximum dominance, during relaxed state, theta wave (4 – 8Hz) [14] shows maximum dominance, during relaxed but attentive state, alpha wave (8 – 12Hz) [15] shows prominence, during cognitive activity, beta wave (12-28 Hz) [16] shows prominence and during meditative state gamma wave (>28 Hz) shows dominance. Though these waves show different levels of activation for different states of consciousness, all waves are present in somewhat superposed fashion for each of those states. Each of these waves have their own characteristic frequency range, spectral power, fluctuation characteristics, entropy, and other properties, which also somewhat depend upon the different states of consciousness.

Background and literature review

The origin, concept and understanding of consciousness is still quite blurry. Right from the time of Aristotle, scholars and philosophers have tried to explore and decode the foundation grounds of consciousness. Aristotle's discussion of perception speaks about two contemporary debates about consciousness: the first, whether consciousness is an intrinsic feature of mental states or a higher-order thought or perception, and the second, concerning the qualitative nature of experience [17]. Over the years, the core concepts have undergone various modifications and consciousness studies have revealed the requirement of deep understanding of different topics of brain sciences [18], including biology, philosophy, quantum mechanics, and psychology, to name a few. Rosenthal [19] reported an elaborate discussion on the connection between mind and consciousness. Any mental state, awake or asleep, alert, or drowsy, is a state of consciousness, which can be studied in details from the electrical and chemical activity and characteristics of the neural waves at play. It is also a long-going debate whether the study of these different states of consciousness involve any quantum mechanical algorithm or not [20] [21]. Since electrical activities in brain reflect the characteristics for different states, study of the neural signals might provide some new and important information. There have been certain studies and attempts to understand the concept of different states of consciousness from extracted EEG signals.

Any state of mind is related with different functioning characteristics of neural signals. Certain early reports discussed about high frequency activity (around 40 Hz activity, i.e., gamma activity) being a neurophysiological correlate of cognition and consciousness [22] [23]. A work by Breschet et al., [24] reported the unique idea of microstate of consciousness, claiming conscious mental activity to be discontinuous and can be represented in form of a series of states of thoughts that manifest as discrete spatiotemporal patterns of global neuronal activity lasting for fractions of seconds, considered as the 'atoms of thought', the basic building blocks or microstates of consciousness. High resolution EEG (62 channel) have been used by Aftanas et al. [25] to study the features of different frequency bands under rest and different altered states of consciousness (different states of meditative stages). A report on transcendental meditation discusses characterization of state of deep relaxation by lowered nervous state arousal and relative deactivation of EEG waves, resulting in slower frequencies of alpha and theta. Certain cases showed increase in theta power of EEG in deep meditative states [26].

Different trends and characteristics of alpha, beta and theta power peaks have been studied and reported [27] during states of deep sleep, transition between waking, NREM and REM etc. An early work [28] was carried out in 1967 with 4 channel EEG, comparing four neural waves (delta, theta, alpha and beta) in different experimental protocols of rest and activity. Certain works have been carried out by Bai et al., on the identification and study of spontaneous transient brain states with help of fMRI (functional magnetic resonance imaging) and magnetoencephalography (MEG) in healthy subjects [29]. Study of consciousness is also related to treatment of various medical conditions like, amnesia or loss of memory [30] [31], brain injury, coma stages, Parkinson's disease [32], Alzheimer patients [33], and various other chronic neural disorders [34]. The blurry line between consciousness, attention, and cognition processes are also another fascinating domain of research [35,36,37,38]. A systematic literature review of 255 EEG-based measures of consciousness in humans have been reported by Nilsen and group [39]. A lot of different kinds of works have been reported, exploring the different brain-states, using different feature extraction tools along with EEG.

A review work was reported by Morrell et al. [40], on new approaches to the field of neural mechanisms in learning with the application of electrophysiological techniques. The wave like properties of alpha wave were discussed by Nuez [41] in 1974. He also discussed in details about the brain wave-equation in another work around the same time [42]. A model of the spatial-temporal characteristics of alpha rhythm were discussed by Rotterdam et al. [43]. A detailed work was reported by Silva, based on experimental findings and theoretical concepts leading to new information regarding mechanisms underlying brain waves [44]. Behaviour of alpha, delta and theta waves for different EEG averaged evoked potentials (AEPs) and event related potentials (ERPs) were discussed by Robinson in a number of works [45] [46].

The Berger effect (change in phase of brain waves) of alpha waves [47] was also another interesting point of study. Different studies regarding oscillations of these waves for different conditions have been extensively reported [48] [49] [50] [51] [52]. Several works have also been reported focusing on different properties of theta waves [53] [54] [55]. Quite a few works have been reported on the travelling property of theta waves [56] [57] [58] [59]. Delta wave activity during sleep has been a topic of deep interest from a long time. Electrophysiological correlates of deep sleep and delta waves have been reported as early as in 1998 [60]. Recent works include delta wave activity during both REM [61] and non-REM sleep [62]. Works regarding power of delta waves have also been reported [63]. Studies correlating sleep and delta waves have been deeply explored by several groups over the years [64] [65] [66] [67] [68].

A lot of debate has been reported in literature on a fundamental question, whether brain behaves non-classically or not. A recent work [69] has shown evidence regarding non-classical functioning of brain, using a witness protocol based on zero quantum coherence (ZQC), which has led to observations of entanglement mediated by consciousness-related brain functions.

Objective of the study

This previous mentioned work [69] has inspired us to study the different properties of three neural waves, delta, theta, and alpha during the resting state of mind. EEG experiment was performed on 7 participants and the neural signals were extracted to compute the parameters chosen for the study. We have tried to study the neural responses using both linear and non-linear modes of computations. Linear property 'Spectral Power' of the delta, theta and alpha components of the extracted EEG responses were computed and compared for both left and right hemispheres of all four lobes. The parameter of 'Power asymmetry' was also computed from the spectral power values, separately for all three waves. Next, using the non-linear technique of MFDFA, complexity of the three waves were computed and compared for both left and right hemisphere of all four lobes, followed by computation of the parameter 'MW asymmetry'. Another measure of complexity, 'Approximate Entropy' was also computed for the three waves. Statistical techniques like One-way ANOVA and Mahalanobis Distance were applied to respectively study the significant difference (if any) between the properties, and nature of distinction between the properties of any two waves at a time (delta-theta, theta-alpha, and delta-alpha).

Analysis Techniques applied

As already mentioned above, we have tried to study, analyze and compare the different neural signals (delta, theta, and alpha), during resting state of 7 voluntary participants. The raw signals

have been extracted with the help of EEG (Electroencephalography) experiment with a procedure explained well in the 'Experimental details' section of the paper.

However, the conventional analysis with linear technique suffers from serious flaws since EEG signals are essentially non-linear and non-stationary, and thus application of non-linear techniques of analysis are more appropriate to examine the finer details of the extracted signals. Otherwise, the results are not expected to provide the deep understanding of neural waves. Detrended Fluctuation Analysis (DFA) has emerged as one of the most widely used techniques [70] to study scaling properties and non-liner correlation detection in non-stationary time series of different kinds. But, in most of bio-signals, one scaling parameter is not sufficient to describe different parts of a signal, which is often characterized by different scaling properties at different instances. The technique of Multifractal Detrended Fluctuation Analysis (MFDFA) [71] is more appropriate for such series, which considers the different scaling behaviour in different part of the signal. This technique studies the detailed long-range correlation and multifractal properties of the given time signal.

This has been widely used in studying earthquake [72], wind measurement [73] [74], meteorological data analysis [75], and even in stock market and finance trend studies [76] [77] [78] [79] etc. This technique explains the scaling properties of the given series with the help of a singularity spectrum, which provides information regarding the different fractal exponents at different parts of the series. The width of the spectrum, known as the multifractal width is a measure of the degree of multifractality, i.e., a measure of the complexity of the signal. We have used this non-linear technique of MFDFA to study the intrinsically embedded fluctuations of the three waves individually, and explain the nature of signal-complexity with help of this parameter. The predictability of the fluctuations in the signals can be further studied by the parameter Approximate Entropy (ApEn) [80] [81], which is another measure of complexity in the signal.

Compared to other methods of scaling analysis like Wavelet Analysis, Discrete Wavelet Transform Approach, WTMM, DMA, MDFA, CDFA etc., MFDFA is more favored technique to analyze non-linear properties of a signal. The simplistic approach and robustness in assessment of signal correlation makes it a more popular choice amongst scientists. It doesn't require modulus maxima procedure, which make programming similar to the conventional DFA method. It also efficiently detects multifractality behaviour in stationary as well a non-stationary time series. Some works have been reported, explaining the advantages of MFDFA over many other techniques [82] [83] [84] [85].

II. EXPERIMENTAL DETAILS

As discussed in the previous section, this study aims at understanding and comparing certain feature behavior and complexity analysis for three neural waves, delta, theta, and alpha during the resting state of consciousness. 7 participants (4 females, 3 males, mean age = 22.3 years) voluntarily offered to take part in the experiments. The experiments were performed at Sir C.V. Raman Centre for Physics and Music, Jadavpur University, Kolkata, West Bengal, India, where subjects were made to sit in comfortable conditions in a dark room. None of the participants have reported any health-related problems during the experiments. The experiment protocol was of approximately 10 minutes' duration, where the participants were asked to sit comfortably in a relaxed state with their eyes closed. No input signal of any kind was applied, and the neural

signals corresponding to this relaxed state was recorded and further analyzed for deeper insights. The details of the experimental set-up and design in discussed in the next section.

EEG experiment

EEG or Electroencephalography [86] [87] [88] is an experiment where neural signals are captured from the scalp portion of a participant in form of electric potentials. These signals get reflected in a screen from where the raw excitations can be extracted and studied further. An EEG cap is placed on the head of the participant, where electrodes are placed in different portions of brain lobes (Fig 1). Odd numbered electrodes refer to left hemispherical zones (F3, F7, T3, T5, P3, O1 etc.) and even-numbered electrodes refer to right hemispherical zones (F4, F8, T4, T6, P4 and O2). A water-soluble AgCl gel is used to establish connection between the electrodes and scalp, from where the neural signal potentials are captured. The position of electrodes on the 10-20 EEG cap is shown in the figure below.

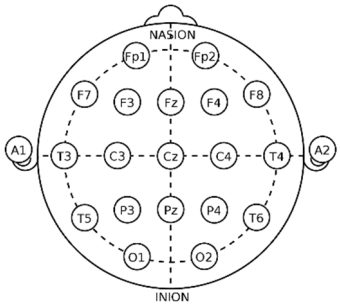

Fig 1. Position of electrode on 10-20 EEG cap

After extraction of the signals, different techniques are applied for analysis of different properties of the extracted signals. In this study, we have used linear techniques to compute properties like Power Spectral and left-right hemispherical Power Asymmetry, as well as, non-linear technique like Multifractal Detrended Fluctuation Analysis (MFDFA) to study the signal complexity of neural signals corresponding to resting state of mind. Approximate Entropy has also been calculated to study the fluctuation nature of the different waves. The detailed feature characteristics have been discussed in the 'Results' and 'Discussions' parts of the paper. All the techniques applied are discussed in the following section of Methodology.

III. METHODOLOGY

i. Pre-processing and denoising EEG data

EEG experiment was performed on 7 participants. The extracted raw EEG signals were filtered with a low and high pass filter with cut-off frequencies of 0.5 to 70 Hz. A notch filter was used to eliminate the electrical interference noise of 50 Hz. High frequency muscle artifacts were removed with the inbuilt EMG filter, which is a second order low pass filter with cut off frequency at 35 Hz (35 Hz double-pole). The EEG data was further cleaned of the low frequency artifacts like minuscule muscular movements and eye blinks with the technique of Empirical Mode Decomposition (EMD). The method elaborately described by Maity et al. [89] has been applied here. EMD decomposes the signal into various artifact free components preserving its

non-linear and non-stationary features to give the noise-free clean EEG signal, which was further analysed by the techniques explained below.

EEG data is a combination of the frequency bands of delta, alpha, theta, beta and gamma. In this work, we have focused on the delta, theta and alpha rhythms of the extracted neural signals. To extract these superposed waves separately along with their respective spectral power values, the technique of Wavelet Transform was next applied on the denoised clean EEG signal.

ii. Wavelet Transform

Wavelet transform (WT) forms a general mathematical tool for signal processing with many applications in EEG data analysis [90] [91] [92] [93]. Time-scale signal analysis and decomposition of EEG signal are few of its primary applications. Here, WT has been used to decompose the raw EEG signal into various frequency bands i.e. delta, alpha, theta, beta etc. The DWT [94] analyzes the signal at different frequency bands with different resolutions by decomposing the signal into a coarse approximation and obtains detailed information. DWT generally employs two sets of functions, called the scaling functions and wavelet functions, associated with low pass and high pass filters, respectively. The decomposition of the signal into different frequency bands is done by successively passing the time-signal through high pass and low pass filters. The original signal x[n] is first passed through a half band high pass filter g[n] and then a low pass filter h[n]. This constitutes one level of decomposition and can mathematically be expressed as follows:

$$y_{high}[k] = \sum x[n] \,.\, g\,[2k-n] \qquad \ldots(i)$$

$$y_{low}[k] = \sum x[n] \,.\, h\,[2k-n] \qquad \ldots(ii)$$

where $y_{high}[k]$ and $y_{low}[k]$ are the outputs of the high pass and low pass filters respectively, after sub sampling by 2. This decomposition halves the time resolution since only half the number of samples now characterizes the entire signal. However, this operation doubles the frequency resolution, since the frequency band of the signal now spans only half the previous frequency band, effectively reducing the uncertainty in the frequency by half. The above procedure, which is also known as the sub band coding, can be repeated for further decomposition [95] [96].

Following the above techniques, clean and denoised delta, theta, and alpha sections were separated from the superposed EEG signals extracted from the frontal (F3, F4, F7, F8), temporal (T3, T4, T5, T6), parietal (P3, P4) and occipital (O1, O2) lobes of all participants, and were further analyzed. The algorithm followed by [97] is used here. Power spectral intensity was calculated separately for delta, theta, and alpha waves. A continuous frequency band from f_{low} to f_{up} was sliced into K bins which can be of equal width or not. Boundaries of bins are specified by a vector band = [f_1, f_2, …..f_K], such that the lower and upper frequencies of the i^{th} bin are f_i and f_{i+1} respectively. The bins used are δ (0.5 – 4 Hz), θ (4 – 7 Hz), and α (8 – 12 Hz). For these bins we have band = [0.5, 4, 7, 12]. The power spectral intensity of the k^{th} bin is evaluated as

$$PSI_k = \sum_{i=|N\left(\frac{f_k}{f_s}\right)|}^{|N\left(\frac{f_{k+1}}{f_s}\right)|} |X_i|^2 \qquad \ldots(iii)$$

where, k=1, 2, …. K-1, f_s is the sampling rate, and N is the series length. Each window was converted into the frequency domain using Fast Fourier Transform (FFT). The average power of delta, theta, and alpha waves, corresponding to the resting state was computed for all the electrodes of all lobes. The error bars give the SD values computed from the different values of spectral power for each electrode.

iii). Calculating Alpha asymmetry

From the power values of different electrodes computed by the technique explained above, asymmetry between left and right portions of each of the four lobes of each participant were next calculated. The well-established concept of frontal alpha asymmetry, introduced by Davidson is applied for the other lobes also. Frontal alpha asymmetry (ALAY) [98] is calculated by the following formula

$$\text{ALAY (A1)} = \ln F4 - \ln F3 \quad \ldots(iv)$$

where lnF4 and lnF3 represent the alpha power of the neural signals of right and left hemispheres of frontal lobe respectively. But, in our experimental set-up, we were able to extract responses for both anterior frontal lobe (F3, F4) as well as posterior frontal lobe (F7, F8). To cover the response of the entire frontal lobe, average alpha power values of all four of these electrodes were calculated to get the overall alpha power values of left and right frontal lobe respectively. The asymmetry value for the whole frontal lobe was then denoted by the following formula:

$$A_f = \ln F_{right} - \ln F_{left} \quad \ldots(v)$$

where, $F_{right} = (F4+F8)/2$, and $F_{left} = (F3+F7)/2$

Following this same technique, power asymmetry was calculated for all other lobes as well.

From respective spectral power values, this power asymmetry value was computed separately for delta, theta, and alpha waves during the state of rest, for all four lobes, frontal, temporal, parietal and occipital.

The two parameters mentioned above are both computed from linear methods of feature analysis. Since EEG signals are both non-linear and non-stationary, application of non-linear signal analysis techniques makes the study more accurate, revealing various interesting and detailed information. Here, we have applied the robust technique of 'Multifractal Detrended Fluctuation Analysis' (MFDFA) to measure the complexity of the underlying fluctuations in the extracted signals, the details of which are explained below.

iv. Computation of Complexity of EEG signal analysis with Multifractal Detrended Fluctuation Analysis (MFDFA)

The technique proposed by Kantelhardt [99] was used to analyze the non-stationary, non-linear EEG signals. This is an efficient method to investigate the long-term correlations present in such signals. The fluctuation function of such a time series follows a power law which is given below.

$$F_q(s) \sim s^{h(q)} \quad \ldots(vi)$$

The scaling behavior of the fluctuation function given above is then calculated by drawing the log-log plot of $F_q(s)$ vs. s for each value of q, where s refers to sample size.

The slope of the log-log plot gives the value of the generalized Hurst exponent H(q) of the signal, which basically is the autocorrelation parameter of the signal, describing the self-similar nature of the signal, by finding out the presence or absence of any kind of long-range temporal correlation. Every monofractal series has a definite Hurst exponent. But most biological signals, like neural signal in this case, are multifractal in nature, and are characterized by multiple Hurst exponents [100]. The range of exponents denote the width of the multifractal spectrum. With the help of least square method [101] [102], the multifractal spectrum can be characterized by a quadratic function fitting about maximum α_0.

$$f(\alpha) = A(\alpha - \alpha_0)^2 + B(\alpha - \alpha_0) + C \quad \ldots(vii)$$

Here C is taken as an additive constant, $C = f(\alpha_0) = 1$ and B is a measure of the asymmetry of the spectrum. For a perfectly symmetric signal, value of B becomes zero. A is a constant which determines the nature or orientation of the obtained spectrum. The width of the spectrum can be obtained by extrapolating the fitted quadratic curve to zero.

Multifractal Width: This multifractal width W is defined as,

$$W = \alpha_1 - \alpha_2 \quad \ldots(viii)$$

with, $f(\alpha_1) = f(\alpha_2) = 0$ …(ix)

A typical multifractal spectrum looks like the figure below.

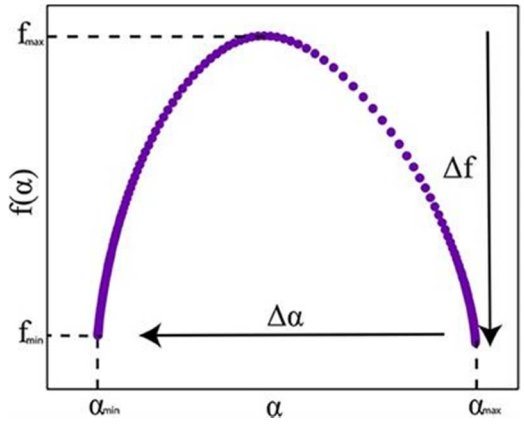

Fig 2. A typical multifractal spectrum

As shown in Fig 2, α_{max} and α_{min} refer to the points α_1 and α_2 in the equation (ix). The width value of the spectrum is thus given by the parameter $\Delta\alpha$, as shown in the figure. The multifractality or complexity of the spectrum is denoted by this multifractal width value. For a monofractal time series, this width gives value zero since h(q) is independent of q in that case.

We have followed the algorithm explained in details by Sanyal et al [103] and Basu et al. [104]. The details of this method of Multifractal Detrended Fluctuation Analysis, along with some related discussions have been reported in Appendix 1.

The inter-hemispherical connectivity for these three waves has been studied next, which is discussed below in details.

iv. Calculating Complexity asymmetry

From the computed results, the 'Multifractal Width' values for electrodes of all lobes were computed for each of the 5 participants, for the three neural waves, delta, theta, and alpha during the resting state of consciousness. Similarly like in case of alpha power, average MW value of right and left hemispheres was computed for each lobe. Multifractal Width (MW) frontal asymmetry ($A_f^{'}$) was calculated using the same technique, i.e., from the difference of complexity values of right and left frontal lobe. The formula is given below:

$$A_f^{'} = MW(F_{right}) - MW(F_{left}) \quad \ldots(x)$$

where, $MW(F_{right}) = MW[(F4+F8)/2]$, and $MW(F_{left}) = MW[(F3+F7)/2]$

The same technique was applied to all other lobes, and the complexity asymmetry of delta, theta, and alpha waves were computed separately for all four lobes, during the resting state of consciousness.

After calculating complexity of the signals, the parameter of Approximate Entropy was next calculated to study the regularity and unpredictability of fluctuations in the signals, i.e., the comparative trend of repetitive fluctuations in all three waves. This parameter, another measure of complexity is explained below.

v. Approximate Entropy (ApEn)

Approximate entropy (ApEn) is a measure of system complexity [105] [106], quantifying the regularity and unpredictability of fluctuations in a signal. A higher value of approximate entropy reflects the possibility that similar patterns of observations are not followed by additional similar observations. In other words, the presence of more repetitive patterns of fluctuations in a time series contributes to the predictability of a signal [107], which is measured by this parameter of ApEn. A time series containing more repetitive patterns has a relatively small ApEn, whereas, a less predictable process has a higher ApEn. The detailed algorithm has been followed from the technique used by Delgado-Bonal et al. [108]. ApEn was initially developed to study and analyze medical data, such as heart rate [109], and over years, it has been widely applied in varied fields of finance [110], physiology [111], climate sciences [112] etc. In later years, it has emerged as a popular tool to characterize and classify EEG signals in patients suffering from schizophrenia [113] [114] [115], epilepsy [116] [117] [118], Parkinson's disease [119] and addiction [120]. We have used this tool of Approximate Entropy, to characterize and analyze the three neural signals, delta, theta, and alpha, extracted during resting state of 7 participant.

v). Statistical tests

From the extracted raw signal, using the above-mentioned technique, feature extraction and computation was performed on delta, theta, and alpha waves, for both left and right hemispherical sections of all four lobes, frontal, temporal, parietal and occipital. Certain tests have also been performed to compare the behavior of three neural waves from a statistical point of view as well. The tools used in the study are discussed briefly below.

a. One-way ANOVA

ANOVA is the technique of analysis of variance [121] [122] [123] [124], where the means or averages of the datasets under study are compared with a definite confidence level (95% in this study) and p value (= 0.05 here) to study how significantly different they are from one another. As discussed above, in this study, we have worked with three neural signals, delta, theta, and alpha. Thus, here one-way ANOVA was performed between the above-mentioned properties (one at a time) of these three signals to study the nature of the significant difference between the waves. This technique was carried out by ORIGIN [125], for each of the EEG parameters discussed above. In case of significant difference between any two waves, the significance value was found to be 1, and in case of no significant difference, this value came to be 0.

b. Mahalanobis distance

In the original variable space, the parameter Mahalanobis Distance gives the measure of the correlation or the divergence or distance [126] between data of various characteristics. It is calculated using the inverse of the variance–covariance matrix of the data set under study. Mahalanobis proposed this measure in 1930, in the context of his studies on racial likeness, and has since then it has proved to be a very important statistical parameter.

Suppose, for two groups labeled as G_1 and G_2, we are interested in studying several relevant characteristics (say p) in both groups. X is defined as a vector which contains all the measurements made of a particular entity and is thus p-dimensional. To compare and classify the two groups, we are often interested in measuring and summarizing their differences. Then the difference between the groups can be considered in terms of the difference between the mean vectors of X, in each group relative to the common within-group variation. This measure is called the Mahalanobis squared distance defined by

$$\Delta^2=(\mu_1-\mu_2)^T\sum^{-1}(\mu_1-\mu_2) \quad \ldots(xii)$$

where 'T' denotes matrix transpose, $\sum$ denotes the common (non-singular) covariance matrix of X in each group G 1 and G_2. Since $\sum$ is a non-singular covariance matrix, it is positive defined and thus Δ is metric. Mahalanobis Δ^2 is mainly used in classification problems, where there are several groups and the investigation concerns the affinities between groups.

In this study, we have calculated M.D. between the feature values of delta, theta, and alpha waves for each lobe separately. A high M.D. value signifies greater distance or divergence between the response distributions of the neural waves, in terms of the properties mentioned before.

IV. RESULTS

i. Spectral power comparison for three neural waves

Delta, theta, and alpha waves have been extracted from the raw neural signal of the rest state of 7 participants, followed by computation of Spectral Power. The plot below shows the comparative power values of the three waves in 4 lobes, in left and right hemispheres separately.

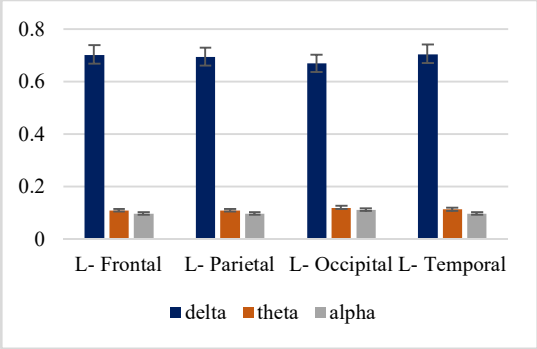

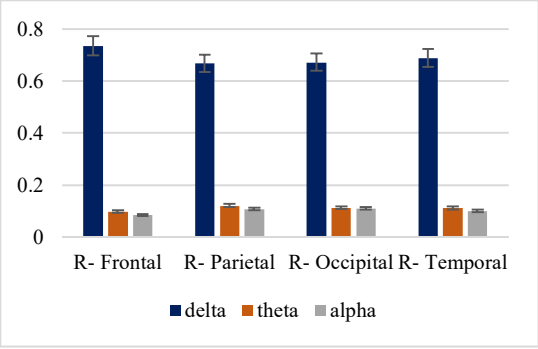

Fig 3a. Spectral power comparison in left hemisphere **Fig 3b**. Spectral power comparison in right hemisphere

Both the hemipsheres show similar trends. Power values for delta waves show distinctly higher values than theta and alpha waves for all four lobes. Theta and alpha waves show almost overlapping power values in all four lobes.

ii. Power asymmetry value comparison for three neural waves

Power asymmetry values have been next calculated for rest state of delta, theta and alpha waves, in all four lobes. The comparative asymmetry values are shown in the plot below.

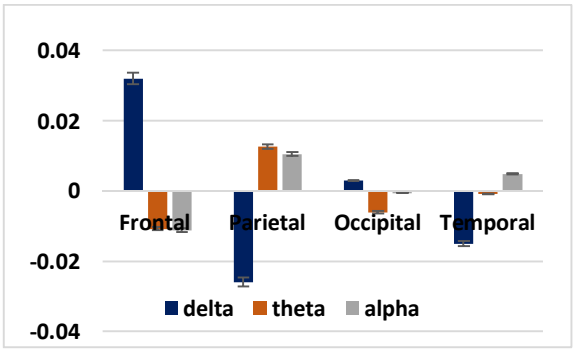

Fig 4. Power asymmetry comparison

Power asymmetry values show different trends in different lobes. In frontal lobe, delta shows maximum asymmetry value, whereas alpha and theta show almost overlapping values. In parietal lobe, theta shows highest value of asymmetry, followed by alpha and delta respectively. In occipital lobe, delta shows the highest value, followed by alpha and theta and in temporal lobe, highest value is shown by alpha, followed by theta and delta.

iii. Complexity value comparison for three neural waves

Next, multifractal width values for the three waves were compared for the resting state of the participants. The results are shown in the plot below.

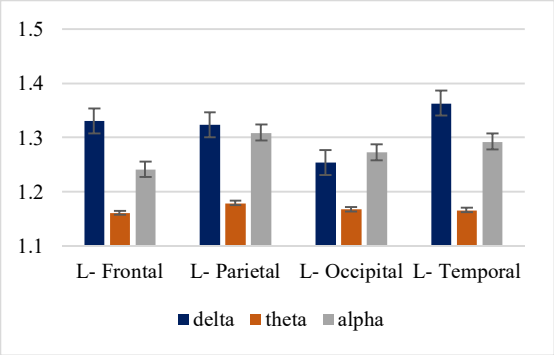

Fig 5a. Complexity comparison in left hemisphere

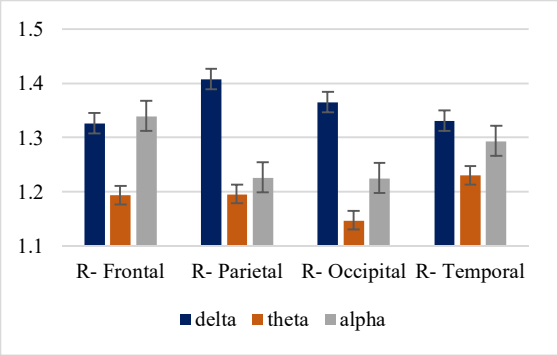

Fig 5b. Complexity comparison in right hemisphere

As can be seen from the plot above, complexity values of the three waves follow a certain trend, similar in both hemispheres of all four lobes. Delta waves show highest complexity values, followed by alpha and theta respectively, in frontal, parietal, and temporal lobe of left hemisphere, and parietal, occipital and temporal lobes of right hemisphere. In left-occipital and right-frontal lobes, alpha shows slightly higher MW values than delta, with minimum value for theta waves.

iv. MW asymmetry value comparison for three neural waves

Similarly, like power asymmetry, MW asymmetry was calculated in rest state for delta, theta and alpha waves for all four lobes, by calculating the complexity difference between right and left hemisphere of each lobe. The comparative picture is shown in the plot below.

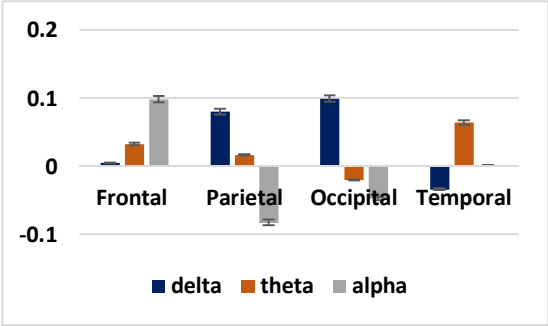

Fig 6. MW asymmetry comparison

Here also, different lobes show different trends of MW asymmetry values for the three neural waves. In frontal lobe, highest value of MW asymmetry was shown by alpha wave, followed by theta and delta. In parietal lobe, highest MW asymmetry was shown by delta, followed by theta and alpha. In occipital lobe, highest MW asymmetry was seen in delta, followed by theta and alpha, and in temporal lobe, highest value was seen in theta, followed by alpha and delta.

v. Entropy value comparison for three neural waves

Next, Approximate Entropy was calculated for all three neural waves in the resting state of the participants, and the comparison is shown in the plot below.

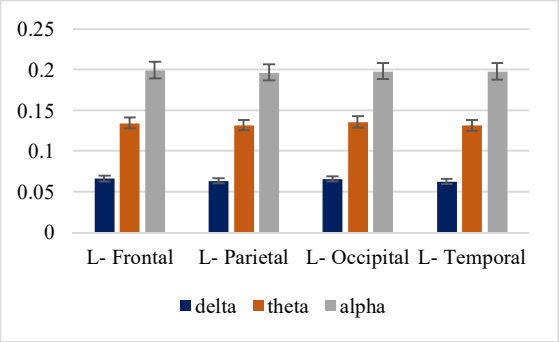

Fig 7a. ApEn comparison in left hemisphere

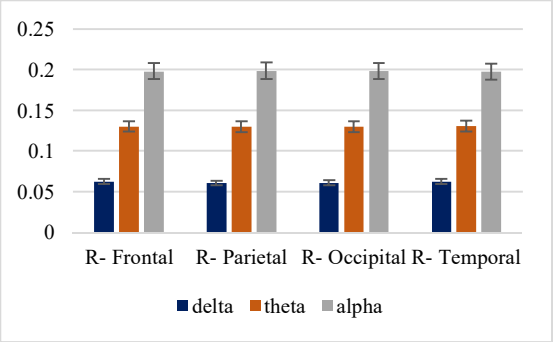

Fig 7b. ApEn comparison in right hemisphere

As can be seen from the plot above, entropy values for delta, theta and alpha waves in resting state follow a certain trend, identical in both hemispheres of all 4 lobes. Maximum ApEn value is shown by alpha waves, followed by theta and delta respectively.

On the computed values of the above explained parameters, statistical tests were performed and the results from each of the tests are explained below.

i. One-way ANOVA

One-way ANOVA was calculated between delta, theta and alpha waves (pair-wise) individually for the parameters spectral power, multifractal width, and ApEn.

a. Spectral Power

		delta-theta	Theta alpha	delta-alpha			delta-theta	theta-alpha	delta-alpha
L- Frontal	F-value	73.33	0.13	66.25	**R- Frontal**	F-value	1.41E+02	0.21	129.24
	Probability	9.17E-08	0.72	1.92E-07		Probability	6.08E-10	0.65	1.20E-09
	Significance	1	0	1		Significance	1	0	1
L- Parietal	F-value	33.68	0.07	30.51	**R-Parietal**	F-value	19.04	0.06	17.37
	Probability	4.04E-04	0.80	5.58E-04		Probability	0.002	0.81	0.003
	Significance	1	0	1		Significance	1	0	1
L-Occipital	F-value	19.22	0.02	17.12	**R-Occipital**	F-value	20.23	0.002	17.36
	Probability	0.002	0.89	0.003		Probability	0.002	0.97	0.003
	Significance	1	0	1		Significance	1	0	1
L-Temporal	F-value	76.18	0.27	69.47	**R-Temporal**	F-value	62.08	0.11	55.84
	Probability	6.94E-08	0.61	1.36E-07		Probability	3.04E-07	0.75	6.38E-07
	Significance	1	0	1		Significance	1	0	1

Table 1a. One-way ANOVA for Spectral Power

Spectral power property of delta waves shows significant difference with that of theta and alpha waves, but no significant difference is seen between power values of theta and alpha waves.

Multifractal width

		delta-theta	theta-alpha	delta-alpha			delta-theta	theta-alpha	delta-alpha
L- Frontal	F-value	9.64	3.25	2.67	**R- Frontal**	F-value	4.97	6.4	0.02
	Probability	0.003	0.07	0.11		Probability	0.03	0.013	0.89
	Significance	1	0	0		Significance	1	1	0
L- Parietal	F-value	2.83	2.76	0.003	**R- Parietal**	F-value	6.89	0.17	6.33
	Probability	0.101	0.11	0.96		Probability	0.01	0.68	0.02
	Significance	0	0	0		Significance	1	0	1
L- Occipital	F-value	1.17	2.40	0.1	**R- Occipital**	F-value	9.07	1.67	2.69
	Probability	0.28	0.13	0.66		Probability	0.004	0.20	0.11
	Significance	0	0	0		Significance	1	0	0
L- Temporal	F-value	9.2	6.24	0.87	**R- Temporal**	F-value	1.82	1.2	0.13
	Probability	0.003	0.015	0.35		Probability	0.18	0.28	0.72
	Significance	1	1	0		Significance	0	0	0

Table 1b. One-way ANOVA for MW value

For left hemispherical section, significant difference is seen in delta-theta pair for frontal and temporal lobes, and for theta-alpha pair in temporal lobe.

For right hemispherical section, significant difference is seen in delta-theta pair for frontal, parietal and occipital lobes, for theta-alpha pair in frontal lobe, and for delta-alpha pair in parietal lobe.

b. Approximate Entropy

		delta-theta	theta-alpha	delta-alpha			delta-theta	theta-alpha	delta-alpha
L- Frontal	F-value	256.8	129.91	801.83	**R- Frontal**	F-value	95.63	73.69	664.83
	Probability	4.24E-12	1.15E-09	2.22E-16		Probability	1.26E-08	8.85E-08	1.11E-15
	Significance	1	1	1		Significance	1	1	1
L- Parietal	F-value	108.25	42.22	287.04	**R- Parietal**	F-value	44.72	30.48	257.19
	Probability	6.31E-06	1.88E-04	1.49E-07		Probability	1.55E-04	5.60E-04	2.29E-07

	Significance	1	1	1		Significance	1	1	1
L-Occipital	F-value	49.62	30.8	273.47	**R-Occipital**	F-value	43.99	29.85	260.81
	Probability	1.08E-04	5.41E-04	1.81E-07		Probability	1.64E-04	5.99E-04	2.17E-07
	Significance	1	1	1		Significance	1	1	1
L-Temporal	F-value	117.31	70.03	642.95	**R-Temporal**	F-value	118.1	73.54	621.06
	Probability	2.58E-09	1.28E-07	1.55E-15		Probability	2.45E-09	8.99E-08	2.11E-15
	Significance	1	1	1		Significance	1	1	1

Table 1c. One-way ANOVA for Approximate Entropy

For the parameter ApEn, in both left and right hemispherical sections, delta-theta, theta-alpha and delta-alpha, all three pairs show significant difference in all four lobes, confirming the fact that ApEn values are significantly different for all three waves in left and right hemispheres of all four lobes.

Next, Mahalanobis Distance was calculated between the three waves, separately for the three parameters spectral power, multifractal width, and ApEn. Plots are shown and explained below.

Mahalanobis Distance

Mahalanobis Distance values between the three waves (pair-wise) for each of the three parameters were separately calculated. Here, trend of M.D. value of each of the parameters is explained in details, along with elaborate bar-graph plots.

a. Spectral power

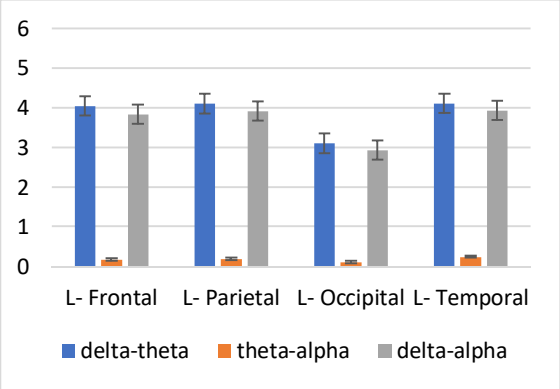

Fig 8a. M.D. for Spectral power in left hemisphere

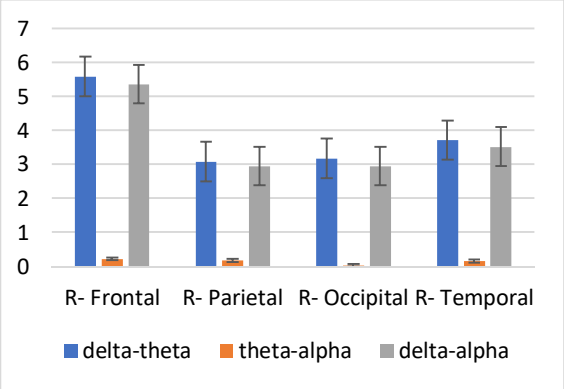

Fig 8b. M.D. for Spectral power in right hemisphere

In case of the parameter Spectral Power, for both left and right hemispheres, the two wave pairs, delta-theta, and delta-alpha, show prominently high distance values in all lobes. The wave pair alpha-theta shows appreciably small distance values in left and right hemispheres of all lobes. Thus, power values of delta waves are seen to be prominently different from that of alpha and

theta waves, but the power values of alpha and theta waves are seen to be much closer, with no appreciable distinction in between.

b. Multifractal Width

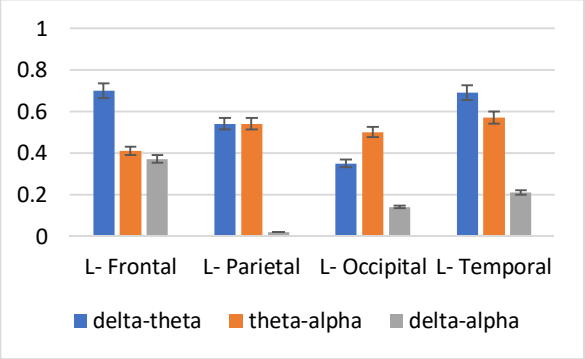

Fig 9a. M.D. for MW in left hemisphere

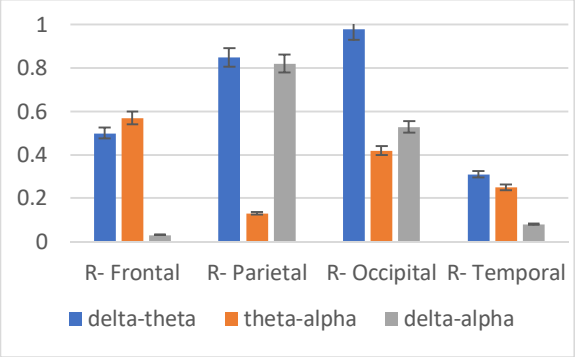

Fig 9b. M.D. for MW in right hemisphere

From the two plots above, the following results can be discussed. In case of the parameter Multifractal Width, for left hemisphere, delta-theta wave pair shows distinctly high M.D. values (> 0.4) in frontal, parietal, and temporal lobes, delta-alpha shows higher values (≈ 0.4) in frontal lobe, with respect to other lobes, and alpha-theta pair shows high values (> 0.4) in all lobes. For right hemisphere, delta-theta wave pair shows distinctly high M.D. values (> 0.4) in frontal, parietal, and occipital lobes, delta-alpha shows high values (> 0.4) in parietal and occipital lobes, and alpha-theta pair shows high values (> 0.4) in frontal and occipital lobes.

Only in left-frontal and right occipital lobes, good distance values between MW value points of all three waves (delta, theta, and alpha) are seen.

c. Approximate Entropy (ApEn)

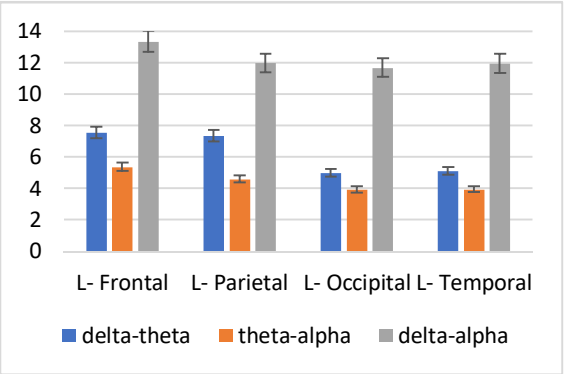

Fig 10a. M.D. for ApEn in left hemisphere

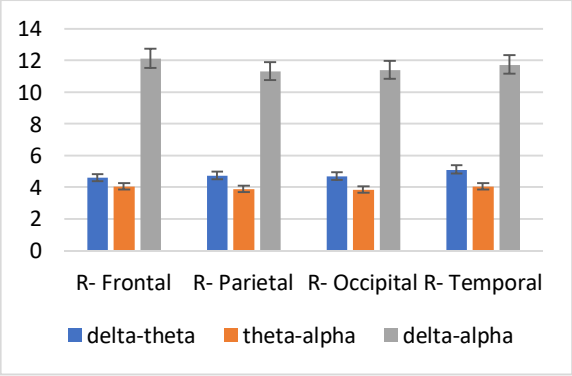

Fig 10b. M.D. for ApEn in right hemisphere

In case of the parameter ApEn, for both left and right hemisphere, prominently high M.D. value is seen for all three wave pairs, maximum for delta-theta pair, followed by delta-theta pair and finally by alpha-theta pair. Thus, ApEn values of all three waves can be considered to be distinctly different from one another.

V. DISCUSSIONS

The entire experiment was carried out for resting state of consciousness of the participants. The aim was to compare and study the trends of different linear and non-linear properties for three neural waves, delta, theta, and alpha, which are all believed to be existing in a superimposed fashion during the resting state, but with varying degree of prominence. The trends of each of the parameters are discussed below in a nutshell, separately for left and right hemispheres of frontal, parietal, occipital, and temporal lobes.

- In both left and right hemispheres of all four lobes, delta waves show prominently higher spectral power than theta and alpha waves. Theta and alpha waves show almost overlapping spectral power values.
- Power spectral asymmetry shows maximum value for delta wave in frontal and occipital lobe, for theta wave in parietal lobe and for alpha wave in temporal lobe.
- In both left and right hemispheres, theta shows lowest values of complexity (multifractal width) in all lobes. Delta shows higher values than alpha in frontal, parietal and temporal lobes of left hemisphere, and, parietal, occipital and temporal lobes of right hemisphere. Only in left-occipital lobe, and right-frontal lobe, alpha shows higher complexity values than delta.
- Multifractal width asymmetry shows maximum value of delta in parietal and occipital lobe, of theta in temporal lobe and of alpha in frontal lobe.
- In both left and right hemisphere of all four lobes, alpha wave shows highest ApEn value, followed by theta and finally delta.

From both the statistical tests of ANOVA and M. Dist. on all three parameters, the following conclusions can be made.

- For the linear property of spectral power, good distinction is seen for delta-theta and delta-alpha pairs in all lobes, whereas no prominent distinction was seen between powers of alpha and theta waves in any lobe.
- For the non-linear parameter of MW, different sections of the brain showed different levels of distinction between the three waves (pair wise), which has been discussed in details in the ‘Results’ part of the paper. Unlike in case of the linear property of Spectral power, MW values of theta and alpha waves showed good distinction in case of left temporal and right-frontal lobes (ANOVA significance value 1 and M. Dist. value > 5.5)
- For ApEn, another measure of complexity of the signal, prominent distinction was seen between all three waves, in all lobes of the brain.

VI. CONCLUSIONS

As can be seen from the results, linear technique of spectral power calculation shows prominently high values of delta waves, but fail to show distinct difference between values of alpha and theta waves in all lobes. Power asymmetry, which is calculated from the spectral power values of the waves in the two hemispheres of all lobes, show overlapping values of alpha and theta waves in frontal and parietal lobes.

Multifractal width, a measure of complexity shows distinct trends for the three waves in different lobes, showing good efficiency of this parameter to study distinction between all the three waves. MW asymmetry, calculated from complexity values of the waves in the two hemispheres of all lobes, show distinctly different values for delta, theta, and alpha waves, making the non-linear technique of MW asymmetry a better choice for neural wave distinction, from the perspective of 'left-right hemispherical asymmetry calculation'.

ApEn, which is another measure of complexity, quantifying the unpredictability of fluctuations or non-linearity in a signal, shows distinct trends for delta, theta, and alpha, making it an efficient distinguishing parameter for these three waves.

It can thus be inferred, that non-linear techniques are more effective to study and distinguish three neural waves, delta, theta, and alpha, and we may emphasize that this investigation clearly indicates that all characteristics of brain waves, in all lobes, are significantly different in delta, theta, and alpha waves which are nothing but manifestation of different states of consciousness. We may thus be prompted to mention, since brain waves have been shown to function non-classically as reported by Kerskens et al. [69], the result of the present work may also be an indication of non-classical nature of consciousness.

Acknowledgement: MB (Ref No D-7/Sc/231/21) acknowledges the Department of Science and Technology (DST), Govt. of India, for providing the DST Inspire Fellowship for this study.

Conflict of Interest: No conflict of interest has been declared by the participating authors of this paper.

Received April 28, 2025; Accepted July 8, 2025

REFERENCES

1. Chayer, Cèline, and Morris Freedman. "Frontal lobe functions." *Current neurology and neuroscience reports* 1.6 (2001): 547-552.
2. Fuster, Joaquín M. "Frontal lobe and cognitive development." *Journal of neurocytology* 31.3 (2002): 373-385.
3. Stuss, Donald T., and Robert T. Knight, eds. *Principles of frontal lobe function*. Oxford University Press, USA, 2013.
4. Squire, Larry R., Craig EL Stark, and Robert E. Clark. "The medial temporal lobe." *Annu. Rev. Neurosci.* 27 (2004): 279-306.
5. Squire, Larry R., and Stuart Zola-Morgan. "The medial temporal lobe memory system." *Science* 253.5026 (1991): 1380-1386.
6. Kiernan, J. A. "Anatomy of the temporal lobe." *Epilepsy research and treatment* 2012 (2012).
7. Critchley, Macdonald. "The parietal lobes." (1953).
8. Denny-Brown, Derek, and R. A. Chambers. "The parietal lobe and behavior." *Research Publications of the Association for Research in Nervous & Mental Disease* (1958).
9. Fogassi, Leonardo, and Giuseppe Luppino. "Motor functions of the parietal lobe." *Current opinion in neurobiology* 15.6 (2005): 626-631.
10. Rehman, Amna, and Yasir Al Khalili. "Neuroanatomy, occipital lobe." (2019).
11. Meyer, Adolf. "The connections of the occipital lobes and the present status of the cerebral visual affections." *Trans Assoc Am Physicians* 22 (1907): 7-16.
12. Amzica, F., and M. Steriade. "Electrophysiological correlates of sleep delta waves." *Electroencephalography and clinical neurophysiology* 107.2 (1998): 69-83.

13. Başar, Erol, et al. "Are cognitive processes manifested in event-related gamma, alpha, theta and delta oscillations in the EEG?." *Neuroscience letters* 259.3 (1999): 165-168.
14. Schacter, Daniel L. "EEG theta waves and psychological phenomena: A review and analysis." *Biological psychology* 5.1 (1977): 47-82.
15. Bazanova, O. M., and D. Vernon. "Interpreting EEG alpha activity." *Neuroscience & Biobehavioral Reviews* 44 (2014): 94-110.
16. Zainuddin, Balkis Solehah, Zakaria Hussain, and Iza Sazanita Isa. "Alpha and beta EEG brainwave signal classification technique: A conceptual study." *2014 IEEE 10th International Colloquium on Signal Processing and its Applications*. IEEE, 2014.
17. Caston, Victor. "Aristotle on consciousness." *Mind* 111.444 (2002): 751-815.
18. Markowitsch, Hans J. "Cerebral bases of consciousness: A historical view." *Neuropsychologia* 33.9 (1995): 1181-1192.
19. Rosenthal, David. *Consciousness and mind*. Clarendon Press, 2005.
20. Stapp, H. P. "In Nature, Cognition and System. Ed. Marc Carvallo." (1992).
21. Penrose, Roger. *Shadows of the Mind*. Vol. 4. Oxford: Oxford University Press, 1994.
22. Joliot, M., U. Ribary, and R. Llinas. "Human oscillatory brain activity near 40 Hz coexists with cognitive temporal binding." *Proceedings of the National Academy of Sciences* 91.24 (1994): 11748-11751.
23. Vanderwolf, C. H. "Are neocortical gamma waves related to consciousness?." *Brain research* 855.2 (2000): 217-224.
24. Bréchet, Lucie, and Christoph M. Michel. "EEG microstates in altered states of consciousness." *Frontiers in Psychology* 13 (2022): 856697.
25. Aftanas, L. I., and S. A. Golosheikin. "Changes in cortical activity in altered states of consciousness: the study of meditation by high-resolution EEG." *Human Physiology* 29 (2003): 143-151.
26. Corby, James C., et al. "Psychophysiological correlates of the practice of Tantric Yoga meditation." *Meditation*. Routledge, 2017. 440-446.
27. Banquet, Jean-Paul, and Maurice Sailhan. "Quantified EEG spectral analysis of sleep and Transcendental Meditation." *Electroencephalography and Clinical Neurophysiology* 42 (1974).
28. Walter, Donald O., J. M. Rhodes, and W. Ross Adey. "Discriminating among states of consciousness by EEG measurements. A study of four subjects." *Electroencephalography and clinical neurophysiology* 22.1 (1967): 22-29.
29. Bai, Yang, et al. "Spontaneous transient brain states in EEG source space in disorders of consciousness." *NeuroImage* 240 (2021): 118407.
30. Markowitsch, Hans J., and Angelica Staniloiu. "Memory, autonoetic consciousness, and the self." *Consciousness and cognition* 20.1 (2011): 16-39.
31. Wilson, Barbara A., Michael Kopelman, and Narinder Kapur. "Prominent and persistent loss of past awareness in amnesia: delusion, impaired consciousness or coping strategy?." *Neuropsychological rehabilitation* 18.5-6 (2008): 527-540.
32. Tangelder, Lousanne EJ, et al. "The value of consciousness coaching in Parkinson's disease: Experiences and possible impact of holistic coaching." *Clinical Parkinsonism & Related Disorders* 10 (2024): 100261.
33. Cooper, E. B., E. J. A. Scherder, and J. B. Cooper. "Electrical treatment of reduced consciousness: experience with coma and Alzheimer's disease." *Neuropsychological rehabilitation* 15.3-4 (2005): 389-405.
34. Bernat, James L. "Chronic disorders of consciousness." *The Lancet* 367.9517 (2006): 1181-1192.
35. De Brigard, Felipe, and Jesse Prinz. "Attention and consciousness." *Wiley interdisciplinary reviews: Cognitive science* 1.1 (2010): 51-59.
36. Koch, Christof, and Naotsugu Tsuchiya. "Attention and consciousness: two distinct brain processes." *Trends in cognitive sciences* 11.1 (2007): 16-22.

37. Dijksterhuis, Ap, and Henk Aarts. "Goals, attention, and (un) consciousness." *Annual review of psychology* 61 (2010): 467-490.
38. Grossberg, Stephen. "The link between brain learning, attention, and consciousness." *Consciousness and cognition* 8.1 (1999): 1-44.
39. Nilsen, André S., et al. "Proposed EEG measures of consciousness: a systematic, comparative review." (2020).
40. Morrell, Frank. "Electrophysiological contributions to the neural basis of learning." *Physiological Reviews* 41.3 (1961): 443-494.
41. Nunez, Paul L. "Wavelike properties of the alpha rhythm." *IEEE Transactions on Biomedical Engineering* 6 (1974): 473-482.
42. Nunez, Paul L. "The brain wave equation: a model for the EEG." *Mathematical Biosciences* 21.3-4 (1974): 279-297.
43. van Rotterdam, 3A, et al. "A model of the spatial-temporal characteristics of the alpha rhythm." *Bulletin of mathematical biology* 44.2 (1982): 283-305.
44. da Silva, Fernando Lopes. "Neural mechanisms underlying brain waves: from neural membranes to networks." *Electroencephalography and clinical neurophysiology* 79.2 (1991): 81-93.
45. Robinson, David L. "The technical, neurological and psychological significance of 'alpha', 'delta' and 'theta'waves confounded in EEG evoked potentials: a study of peak latencies." *Clinical Neurophysiology* 110.8 (1999): 1427-1434.
46. Robinson, David L. "The technical, neurological, and psychological significance of 'alpha','delta'and 'theta'waves confounded in EEG evoked potentials: a study of peak amplitudes." *Personality and Individual Differences* 28.4 (2000): 673-693.
47. Kirschfeld, Kuno. "The physical basis of alpha waves in the electroencephalogram and the origin of the "Berger effect"." *Biological cybernetics* 92.3 (2005): 177-185.
48. Alamia, Andrea, and Rufin VanRullen. "Alpha oscillations and traveling waves: Signatures of predictive coding?." *PLoS Biology* 17.10 (2019): e3000487.
49. Bazanova, O. M., and D. Vernon. "Interpreting EEG alpha activity." *Neuroscience & Biobehavioral Reviews* 44 (2014): 94-110.
50. Zhang, Honghui, et al. "Theta and alpha oscillations are traveling waves in the human neocortex." *Neuron* 98.6 (2018): 1269-1281.
51. Cantero, Jose L., Mercedes Atienza, and Rosa M. Salas. "Human alpha oscillations in wakefulness, drowsiness period, and REM sleep: different electroencephalographic phenomena within the alpha band." *Neurophysiologie Clinique/Clinical Neurophysiology* 32.1 (2002): 54-71.
52. Schürmann, Martin, and Erol Başar. "Functional aspects of alpha oscillations in the EEG." *International Journal of Psychophysiology* 39.2-3 (2001): 151-158.
53. Artemenko, D. P. "Role of hippocampal neurons in theta-wave generation." *Neurophysiology* 4.5 (1972): 409-415.
54. Tsodyks, Misha V., et al. "Population dynamics and theta rhythm phase precession of hippocampal place cell firing: a spiking neuron model." *Hippocampus* 6.3 (1996): 271-280.
55. Goyal, Abhinav, et al. "Functionally distinct high and low theta oscillations in the human hippocampus." *Nature communications* 11.1 (2020): 2469.
56. Zhang, Honghui, and Joshua Jacobs. "Traveling theta waves in the human hippocampus." *Journal of Neuroscience* 35.36 (2015): 12477-12487.
57. Zhang, Honghui, et al. "Theta and alpha oscillations are traveling waves in the human neocortex." *Neuron* 98.6 (2018): 1269-1281.
58. Lubenov, Evgueniy V., and Athanassios G. Siapas. "Hippocampal theta oscillations are travelling waves." *Nature* 459.7246 (2009): 534-539.
59. Patten, Timothy M., et al. "Human cortical traveling waves: dynamical properties and correlations with responses." *PLoS One* 7.6 (2012): e38392.

60. Amzica, F., and M. Steriade. "Electrophysiological correlates of sleep delta waves." *Electroencephalography and clinical neurophysiology* 107.2 (1998): 69-83.
61. Bernardi, Giulio, et al. "Regional delta waves in human rapid eye movement sleep." *Journal of Neuroscience* 39.14 (2019): 2686-2697.
62. Dang-Vu, Thien Thanh, et al. "Cerebral correlates of delta waves during non-REM sleep revisited." *Neuroimage* 28.1 (2005): 14-21.
63. Davis, Christopher J., et al. "Delta wave power: an independent sleep phenotype or epiphenomenon?." *Journal of clinical sleep medicine* 7.5 Suppl (2011): S16-S18.
64. Pilon, Mathieu, et al. "Hypersynchronous delta waves and somnambulism: brain topography and effect of sleep deprivation." *Sleep* 29.1 (2006): 77-84.
65. Lanquart, Jean-Pol, et al. "The dichotomy between low frequency and delta waves in human sleep: a reappraisal." *Journal of neuroscience methods* 293 (2018): 234-246.
66. Smith, J. R., I. Karacan, and M. Yang. "Ontogeny of delta activity during human sleep." *Electroencephalography and clinical neurophysiology* 43.2 (1977): 229-237.
67. Lee, Jungryun, Daesoo Kim, and Hee-Sup Shin. "Lack of delta waves and sleep disturbances during non-rapid eye movement sleep in mice lacking α1G-subunit of T-type calcium channels." *Proceedings of the National Academy of Sciences* 101.52 (2004): 18195-18199.
68. Sekimoto, Masanori, et al. "Asymmetric interhemispheric delta waves during all-night sleep in humans." *Clinical neurophysiology* 111.5 (2000): 924-928.
69. Kerskens, Christian Matthias, and David López Pérez. "Experimental indications of non-classical brain functions." *Journal of Physics Communications* 6.10 (2022): 105001.
70. Peng, C-K., et al. "Mosaic organization of DNA nucleotides." *Physical review e* 49.2 (1994): 1685.
71. Kantelhardt, J. W., Koscielny-Bunde, E., Rego, H. H., Havlin, S., & Bunde, A. (2001). Detecting long-range correlations with detrended fluctuation analysis. *Physica A: Statistical Mechanics and its Applications*, *295*(3-4), 441-454.
72. Alam, A., Wang, N., Petraki, E., Barkat, A., Huang, F., Shah, M. A., ... & Nikolopoulos, D. (2021). Fluctuation Dynamics of Radon in Groundwater Prior to the Gansu Earthquake, China (22 July 2013: M s= 6.6): Investigation with DFA and MFDFA Methods. *Pure and Applied Geophysics*, *178*(9), 3375-3395.
73. Telesca, L., Lovallo, M., & Kanevski, M. (2016). Power spectrum and multifractal detrended fluctuation analysis of high-frequency wind measurements in mountainous regions. *Applied energy*, *162*, 1052-1061.
74. Stosic, Tatijana, Luciano Telesca, and Borko Stosic. "Multiparametric statistical and dynamical analysis of angular high-frequency wind speed time series." *Physica A: Statistical Mechanics and its Applications* 566 (2021): 125627.
75. Baranowski, P., Krzyszczak, J., Slawinski, C., Hoffmann, H., Kozyra, J., Nieróbca, A., ... & Gluza, A. (2015). Multifractal analysis of meteorological time series to assess climate impacts. *Climate Research*, *65*, 39-52.
76. Miloș, L. R., Hațiegan, C., Miloș, M. C., Barna, F. M., & Boțoc, C. (2020). Multifractal detrended fluctuation analysis (MF-DFA) of stock market indexes. Empirical evidence from seven central and eastern European markets. *Sustainability*, *12*(2), 535.
77. Zunino, L., Tabak, B. M., Figliola, A., Pérez, D. G., Garavaglia, M., & Rosso, O. A. (2008). A multifractal approach for stock market inefficiency. *Physica A: Statistical Mechanics and its Applications*, *387*(26), 6558-6566.
78. Grech, D. (2016). Alternative measure of multifractal content and its application in finance. *Chaos, solitons & fractals*, *88*, 183-195.
79. Zunino, L., Figliola, A., Tabak, B. M., Pérez, D. G., Garavaglia, M., & Rosso, O. A. (2009). Multifractal structure in Latin-American market indices. *Chaos, Solitons & Fractals*, *41*(5), 2331-2340.

80. Burioka, N., Miyata, M., Cornélissen, G., Halberg, F., Takeshima, T., Kaplan, D. T., ... & Shimizu, E. (2005). Approximate entropy in the electroencephalogram during wake and sleep. *Clinical EEG and neuroscience*, *36*(1), 21-24.
81. Srinivasan, V., Eswaran, C., & Sriraam, N. (2007). Approximate entropy-based epileptic EEG detection using artificial neural networks. *IEEE Transactions on information Technology in Biomedicine*, *11*(3), 288-295.
82. Oświęcimka, Paweł, et al. "Detrended cross-correlation analysis consistently extended to multifractality." *Physical Review E* 89.2 (2014): 023305.
83. Serrano, Eduardo, and Alejandra Figliola. "Wavelet leaders: a new method to estimate the multifractal singularity spectra." *Physica A: Statistical Mechanics and its Applications* 388.14 (2009): 2793-2805.
84. Figliola, Alejandra, et al. "About the effectiveness of different methods for the estimation of the multifractal spectrum of natural series." *International Journal of Bifurcation and chaos* 20.02 (2010): 331-339.
85. Huang, Y. X., et al. "Arbitrary-order Hilbert spectral analysis for time series possessing scaling statistics: Comparison study with detrended fluctuation analysis and wavelet leaders." *Physical Review E—Statistical, Nonlinear, and Soft Matter Physics* 84.1 (2011): 016208.
86. Kirschstein, Timo, and Rüdiger Köhling. "What is the source of the EEG?." *Clinical EEG and neuroscience* 40.3 (2009): 146-149.
87. Teplan, Michal. "Fundamentals of EEG measurement." *Measurement science review* 2.2 (2002): 1-11.
88. Cooper, Raymond, John Walkinshaw Osselton, and John Crossley Shaw. *EEG technology*. Butterworth-Heinemann, 2014.
89. Maity, Akash Kumar, et al. "Multifractal detrended fluctuation analysis of alpha and theta EEG rhythms with musical stimuli." *Chaos, Solitons & Fractals* 81 (2015): 52-67.
90. Selesnick, Ivan W., Richard G. Baraniuk, and Nick C. Kingsbury. "The dual-tree complex wavelet transform." *IEEE signal processing magazine* 22.6 (2005): 123-151.
91. Dimoulas, Charalampos, et al. "Long-term signal detection, segmentation and summarization using wavelets and fractal dimension: A bioacoustics application in gastrointestinal-motility monitoring." *Computers in Biology and Medicine* 37.4 (2007): 438-462.
92. Hazarika, Neep, et al. "Classification of EEG signals using the wavelet transform." *Signal processing* 59.1 (1997): 61-72.
93. Adeli, H., Zhou, Z., & Dadmehr, N. (2003). Analysis of EEG records in an epileptic patient using wavelet transform. *Journal of neuroscience methods*, *123*(1), 69-87.
94. Akin, M., et al. "A new approach for diagnosing epilepsy by using wavelet transform and neural networks." *2001 Conference Proceedings of the 23rd Annual International Conference of the IEEE Engineering in Medicine and Biology Society*. Vol. 2. IEEE, 2001.
95. Sivanandam, S. N., Sai Sumathi, and S. N. Deepa. "Introduction to neural networks using Matlab 6.0." *(No Title)* (2006).
96. Mehrotra, Kishan, Chilukuri K. Mohan, and Sanjay Ranka. *Elements of artificial neural networks*. MIT press, 1997.
97. Sanyal, Shankha, et al. "Detrended fluctuation and power spectral analysis of alpha and delta EEG brain rhythms to study music elicited emotion." *2015 International Conference on Signal Processing, Computing and Control (ISPCC)*. IEEE, 2015.
98. Davidson, Richard J. "What does the prefrontal cortex "do" in affect: perspectives on frontal EEG asymmetry research." *Biological psychology* 67.1-2 (2004): 219-234.
99. Kantelhardt, Jan W., et al. "Multifractal detrended fluctuation analysis of nonstationary time series." *Physica A: Statistical Mechanics and its Applications* 316.1-4 (2002): 87-114.
100. Ashkenazy, Yosef, et al. "Nonlinearity and multifractality of climate change in the past 420,000 years." *Geophysical research letters* 30.22 (2003).
101. Axelsson, Owe. "A generalized conjugate gradient, least square method." *Numerische Mathematik* 51.2 (1987): 209-227.

102. Figliola, A., et al. "Study of EEG brain maturation signals with multifractal detrended fluctuation analysis." *AIP conference proceedings*. Vol. 913. No. 1. American Institute of Physics, 2007.
103. Nag, Sayan, et al. "On the application of deep learning and multifractal techniques to classify emotions and instruments using Indian Classical Music." *Physica A: Statistical Mechanics and its Applications* 597 (2022): 127261.
104. Basu, Medha, et al. "Neural quantification of timbre and emotions from Indian Classical Music: A multifractal exploration." *Physica A: Statistical Mechanics and its Applications* 624 (2023): 128937.
105. Pincus, Steven M. "Approximate entropy as a measure of system complexity." *Proceedings of the national academy of sciences* 88.6 (1991): 2297-2301.
106. Pincus, Steve. "Approximate entropy (ApEn) as a complexity measure." *Chaos: An Interdisciplinary Journal of Nonlinear Science* 5.1 (1995): 110-117.
107. Ho, K. K., Moody, G. B., Peng, C. K., Mietus, J. E., Larson, M. G., Levy, D., & Goldberger, A. L. (1997). Predicting survival in heart failure case and control subjects by use of fully automated methods for deriving nonlinear and conventional indices of heart rate dynamics. *Circulation*, *96*(3), 842-848.
108. Delgado-Bonal, Alfonso, and Alexander Marshak. "Approximate entropy and sample entropy: A comprehensive tutorial." *Entropy* 21.6 (2019): 541.
109. Pincus, Steven M., Igor M. Gladstone, and Richard A. Ehrenkranz. "A regularity statistic for medical data analysis." *Journal of clinical monitoring* 7 (1991): 335-345.
110. Pincus, S., & Kalman, R. E. (2004). Irregularity, volatility, risk, and financial market time series. *Proceedings of the National Academy of Sciences*, *101*(38), 13709-13714.
111. Pincus, Steven M., and Ary L. Goldberger. "Physiological time-series analysis: what does regularity quantify?." *American Journal of Physiology-Heart and Circulatory Physiology* 266.4 (1994): H1643-H1656.
112. Delgado-Bonal, Alfonso, et al. "Analyzing changes in the complexity of climate in the last four decades using MERRA-2 radiation data." *Scientific reports* 10.1 (2020): 922.
113. Sabeti, Malihe, Serajeddin Katebi, and Reza Boostani. "Entropy and complexity measures for EEG signal classification of schizophrenic and control participants." *Artificial intelligence in medicine* 47.3 (2009): 263-274.
114. Peupelmann, J., Boettger, M. K., Ruhland, C., Berger, S., Ramachandraiah, C. T., Yeragani, V. K., & Bär, K. J. (2009). Cardio-respiratory coupling indicates suppression of vagal activity in acute schizophrenia. *Schizophrenia research*, *112*(1-3), 153-157.
115. Sabeti, M., Behroozi, R., & Moradi, E. (2016). Analysing complexity, variability and spectral measures of schizophrenic EEG signal. *International Journal of Biomedical Engineering and Technology*, *21*(2), 109-127.
116. Yuan, Q., Zhou, W., Li, S., & Cai, D. (2011). Epileptic EEG classification based on extreme learning machine and nonlinear features. *Epilepsy research*, *96*(1-2), 29-38.
117. Kumar, Y., Dewal, M. L., & Anand, R. S. (2014). Epileptic seizures detection in EEG using DWT-based ApEn and artificial neural network. *Signal, Image and Video Processing*, *8*, 1323-1334.
118. Ocak, H. (2009). Automatic detection of epileptic seizures in EEG using discrete wavelet transform and approximate entropy. *Expert Systems with Applications*, *36*(2), 2027-2036.
119. Pappalettera, C., Miraglia, F., Cotelli, M., Rossini, P. M., & Vecchio, F. (2022). Analysis of complexity in the EEG activity of Parkinson's disease patients by means of approximate entropy. *GeroScience*, *44*(3), 1599-1607.
120. Yun, K., Park, H. K., Kwon, D. H., Kim, Y. T., Cho, S. N., Cho, H. J., ... & Jeong, J. (2012). Decreased cortical complexity in methamphetamine abusers. *Psychiatry Research: Neuroimaging*, *201*(3), 226-232.
121. Miller Jr, R. G. (1997). *Beyond ANOVA: basics of applied statistics*. CRC press.
122. St, Lars, and Svante Wold. "Analysis of variance (ANOVA)." *Chemometrics and intelligent laboratory systems* 6.4 (1989): 259-272.

123. Stevenson, Keith J. "Review of originpro 8.5." *Journal of the American Chemical Society* 133.14 (2011): 5621.
124. Kim, Tae Kyun. "Understanding one-way ANOVA using conceptual figures." *Korean journal of anesthesiology* 70.1 (2017): 22-26.
125. Ross, Amanda, et al. "One-way anova." *Basic and advanced statistical tests: Writing results sections and creating tables and figures* (2017): 21-24.
126. McLachlan, Goeffrey J. "Mahalanobis distance." *Resonance* 4.6 (1999): 20-26.
127. Banerjee, Archi, et al. "A novel study on perception–cognition scenario in music using deterministic and non-deterministic approach." *Physica A: Statistical Mechanics and its Applications* 567 (2021): 125682.
128. Sanyal, Shankha, et al. "Tagore and neuroscience: A non-linear multifractal study to encapsulate the evolution of Tagore songs over a century." *Entertainment Computing* 37 (2021): 100367.
129. Sanyal, S., Banerjee, A., Patranabis, A., Banerjee, K., Sengupta, R., & Ghosh, D. (2016). A study on improvisation in a musical performance using multifractal detrended cross correlation analysis. *Physica A: Statistical Mechanics and its Applications*, *462*, 67-83.
130. Kwapień, Jarosław, et al. "Genuine multifractality in time series is due to temporal correlations." *Physical Review E* 107.3 (2023): 034139.

APPENDIX 1

Multifractal Detrended Fluctuation Analysis (MFDFA)

Matlab programming has been used to perform the whole procedure, the steps of which are explained below:

- **Step 1** – Converting the complex signal into a simpler one Y(i), by deducting the mean value of the signal form every instant of the signal

$$Y(i) = \sum (x_k - x') \quad \ldots(i)$$

Where, x' is the mean value of the signal

- **Step 2** – The whole signal Y(i) is divided into Ns segments, with a certain number of samples. With sample size s and the length of the whole signal N, the segments are denoted as

$$Ns = \text{int}(N/s) \quad \ldots(ii)$$

- **Step 3 –** The local RMS variation for sample size s is denoted by the function F(s,v), which is explained below:

$$F^2(s,v) = \frac{1}{s}\sum_{i=1}^{s}\{Y[(v-1)s+i] - y_v(i)\}^2 \quad \ldots(iii)$$

- **Step 4 –** The q-order overall RMS variation for different scale sized obtained by using the following formula:

$$F_q(s) = \{\frac{1}{Ns}\sum_{v=1}^{Ns}[F^2(s,v)]^{\frac{q}{2}}\}^{\frac{1}{q}} \quad \ldots(iv)$$

- **Step 5** – The scaling behavior of the fluctuation function given above is calculated by drawing the log-log plot of $F_q(s)$ vs. s for each value of q **(Fig. 2a and b)**. The following equation is obtained from the plot:

$$F_q(s) \sim s^{h(q)} \quad \ldots(v)$$

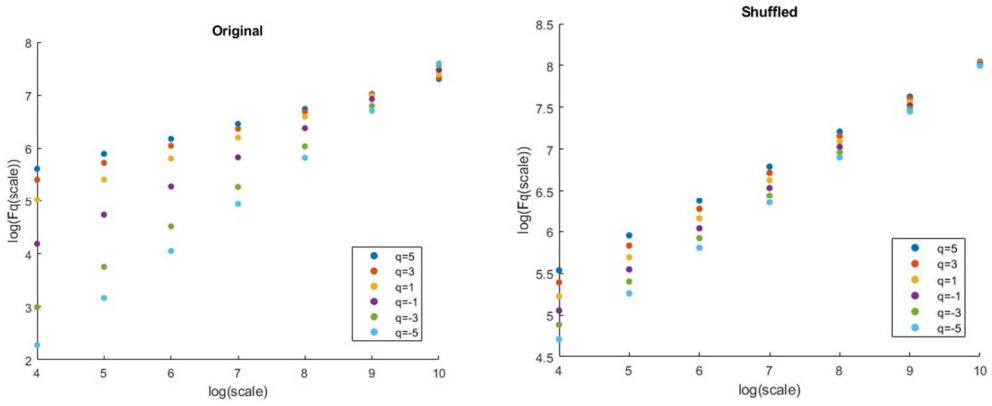

Fig 2(a) **Fig 2(b)**

Fig 2(a, b): $\log_2$ (F_q(scale)) vs $\log_2$(scale) plot for original and shuffled series for a definite participant's EEG response of electrode F8 corresponding to resting state

Fig. 2(a) and **(b)** show the regression plots of F(s) vs (s) for ''original'' and ''randomly shuffled'' time series of the F8 electrode EEG response (alpha wave) of a participant, corresponding to resting state. The values of h(q) are obtained from the slope of the best fit line obtained from $\log_2 F_q(s)$ vs $\log_2$ (scale) plot. This parameter h(q) is called the generalized Hurst exponent, which is the measure of self-similarity and correlation properties of the time series under study. The presence or absence of long-range correlation within a signal is given by the value of this Hurst exponent. A monofractal time series has a unique value of h(q) for all values of q. **Fig. 2(c)** shows the variation of h(q) vs q for an original and shuffled multifractal series for the same conditions.

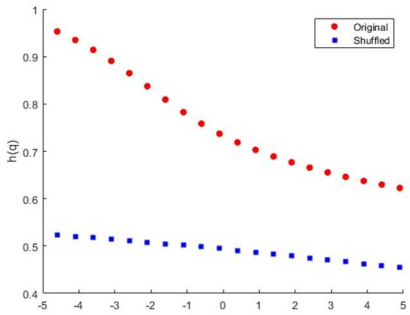

Fig 2(c): Sample h(q) vs (q) plot for "original" and "shuffled" series for a definite participant's EEG response of electrode F8 corresponding to resting state

In **Fig. 2(c),** q is plotted for 10 points in between −5 to +5. The origin of multifractality in the neural signal can be verified by shuffling the original time series data randomly [127] [128] [129]. This process of random shuffling destroys all the existing long-range correlations in the original data and results in a completely uncorrelated sequence.

This generalized Hurst exponent H(q) of MFDFA is related to the classical exponent τ(q) by the following equation:

$$\tau(q) = qh(q) - 1 \qquad \ldots(vi)$$

For a monofractal series with long range correlation has a linearly dependent q order exponent τ(q) with a single unique Hurst exponent h. But, in case of multifractal signal, τ(q) depends non-linearly on q and the signal is characterized by multiple Hurst exponents [100].

The singularity spectrum f(α) is related to the Hurst exponent h(q) by the following equation:

$$\alpha = h(q) + qh'(q) \quad \ldots(vii)$$
$$f(\alpha) = q[\alpha - h(q)] + 1 \quad \ldots(viii)$$

Where, α denotes the singularity strength and f(α) denotes the dimension of subset series, characterized by α. The range of exponents denote the width of the multifractal spectrum. With the help of least square method [101] [102], the multifractal spectrum can be characterized by fitting a quadratic function in the neighborhood of maximum α_0.

$$f(\alpha) = A(\alpha - \alpha_0)^2 + B(\alpha - \alpha_0) + C \quad \ldots(ix)$$

Here C is taken as an additive constant, $C = f(\alpha_0) = 1$ and B is a measure of the asymmetry of the spectrum. Value of B becomes zero for a perfectly symmetric signal. A is a constant which determines the nature or orientation of the obtained spectrum. The width of the spectrum can be obtained by extrapolating the fitted quadratic curve to zero.

Following the steps discussed above, the multifractal spectrums of each of the subjects for the clips under experiment were plotted. From the spectrum, the following parameters were computed to for a detailed analysis of the nature of the recorded EEG signals.

a. ***Multifractal Width:*** This multifractal width W is defined as,

$$W = \alpha_1 - \alpha_2 \ldots(x)$$
$$\text{with,} \quad f(\alpha_1) = f(\alpha_2) = 0 \quad \ldots(xi)$$

The multifractality of the spectrum is denoted by this multifractal width value. In other words, this width value gives the measure of complexity of the signal. For a monofractal time series, this width gives value zero since h(q) is independent of q in that case.

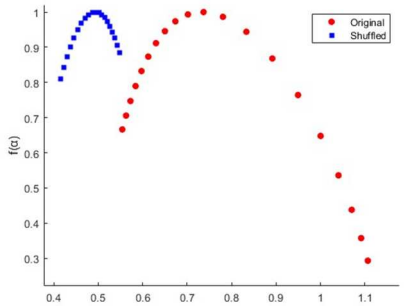

Fig 2(d): f(α) vs α plot for original and shuffled series for a definite participant's EEG response of electrode F8 corresponding to resting state

Fig. 2(c) shows the variation of h(q) vs q and **Fig. 2(d)** shows the variation of f(α) vs α for an original and shuffled multifractal series for the same conditions. The fluctuation function obtained from the shuffled series exhibits simple random behavior, with the slope corresponding to $h_{shuf}(q)$=0.5, i.e., nonmultifractal scaling. In the fluctuation function obtained from the shuffled series, it exhibits simple random behavior, with the slope corresponding to $h_{shuf}(q) \sim 0.5$, i.e., non-multifractal scaling. This implies that the multifractality obtained in this case can be due to different long-range correlations for small as well as large fluctuations.

If the multifractality of the original data is due to long range correlations, the shuffled data will show non-fractal scaling, i.e., the self-similar nature of the signal would be absent. On the other hand, if the initial h(q) dependence does not change, i.e., if $h(q) = h_{shuffled}(q)$, then the origin of multifractality is not due to the presence of long-range correlations in the signal, but because of broad probability density function of the time series. If any series has multifractality both due to long range correlation as well as probability density function, then the shuffled series will have smaller width W than the original series.

From the shown figure, the variation of h(q) with q clearly indicates a multifractal behavior for EEG alpha waves, as the shuffled values show remarkable difference from that of the original values. Also, only if small and large fluctuations scale differently, there will be significant dependence of h(q) on q, indicating multifractal nature. While considering negative values of q, we focus our attention to the smaller fluctuations and hence higher values of scaling exponent, while for positive values of q, we focus our attention to the larger fluctuations and hence smaller values of h(q). It is also evident from the figures that in most cases the values of h(q) decrease with increasing q which as another evidence of multifractality in the time series. On the other hand, the for the shuffled series, h(q) shows very little variation or sometimes no variation with q, showing monofractal behavior, since all the long-range correlations are destroyed during random shuffling of the time series data.

Ideally, the shuffled series spectrum, which is devoid of any correlation, should have had zero width. But as can be seen in the figure above (Fig 2d), the shuffled spectrum shows some finite width. This is due to 'finite size effect' of the time series under study here.

Kwapien et al. [130] explains the non-zero width of shuffled spectrum very systematically. When the number of data points of a time series tend towards infinity, the width of the shuffled series ultimately reduces to zero, thus leading to a monofractal series (or a bifractal series in case of Levy-basin of attraction). The power laws explaining uncorrelated series, with thinner tails of probability distribution functions such that they are Levy-unstable, belong to the Gaussian basin of attraction, and lead to monofractal dynamics, if the number of date points can be extended to infinity. This work is not a case of Levy basin of attraction, and thus will lead to monofractal dynamics after shuffling, for sufficiently large number of data points.

The procedure of shuffling destroys all the correlations in the time series, thus making the neighborhood random. All the Hölder exponents (α) are expected to approach 0.5 thus destroying the existing correlations in the series. But, for a finite time series, it is natural to find some related dispersion of its values at around 0.5, which is seen in case of some numerical analyses. This carries no contribution to the existence of multifractality in the series, and can be considered as an apparent effect of the short scale of the series. In real world experiments, it is not possible to achieve infinite numbers of data points in the time series, which is the reason behind the non-zero width of the shuffled spectrum.